Nigerian Journal of Physics (NJP)

ISSN: 1595-0611

Volume 32(1), March 2023

Computational Study of Structural Transformation in Densified Silica glass

***Igwe, I. E., Sule, Z. B.**

Department of Physics, Federal University Dusin-Ma, Katsina State. Nigeria

*Corresponding author's email: iigwe@fudutsinma.edu.ng

ABSTRACT

Pressure-induced change in structure and properties of noncrystalline materials, such as liquids and glasses, is an important and challenging issue in condensed-matter physics. In this study, molecular dynamics (MD) was used to provide insight into the microscopic picture of changes in the structural correlation of densified SiO_2 glass. The simulations are based on the effective interatomic potential. Changes in the position and height of the first sharp peak in the pair distribution function and bond-angle distributions were investigated as a function of density. The pair-distribution function show that the average Si-O bond length at normal density is 1.62 Å, then linearly increases to 1.67 Å at high density. At high density where the glass reaches the stishovite density the Si-O coordination changes from 4 to 5.8 and the O-Si-O angle distribution is peaked at 90° with a full width at half maximum (FWHM) of 21° and the Si-O-Si angle distribution is peaked at 95° and 128°. The Si-O bond angle distribution becomes covalent-like and the O-Si-O bond angle distribution becomes broader upon densification. These results provide firm evidence that the system has transformed from a corner-sharing tetrahedral network to one in which there are corner-sharing and edge-sharing octahedral.

Keywords:
Silica glass,
Molecular dynamics simulation,
High pressure,
Oxide glass.

INTRODUCTION

Silica (SiO_2) is a common material which is of great importance in chemistry, geology and industrial applications. It is the fundamental building block of three-dimensional framework structure found in minerals. Under ambient conditions, the structures are based on a relatively open arrangement of corner sharing tetrahedral units with four oxygen atoms surrounding a central silicon atom (Du, et al., 2022). Silica (SiO_2), is particularly interesting due to its many polymorphs: β-cristobalite (cubic), α-quartz (trigonal), and β-quantz (hexagonal), coesite and stishovite (Brazhkin, et al., 2011; Klinger, 2013; Machon, et al., 2014)

In crystalline state, silica exists in a variety of polymorphic form with varying densities. Experimental and theoretical studies (Grimsditch, 1986; Hong & Newville, 2020; Kapoor, et al., 2017; Polian & Grimsditch, 1990), have concluded SiO_2 undergo a number of structural transformation with varying temperature and pressure. For example, low-temperature quartz (α-quartz) undergoes a structural transformation into the high β-quantz. At room temperature, quartz changes into coesite with a slight increase in pressure. With further increase in pressure, coesite transforms into stishovite. In contrast to transitions in crystals, the structural order of amorphous SiO_2 can be divided into intermediate-range order (IRO) i.e. through the alteration of the interatomic distance between silicon and surrounding oxygen atoms and short range order (SRO) in the glass.

It is well known that at ambient conditions, silica glass exhibit corner-sharing $Si(O_{1/2})_4$ tetrahedral in normal density (2.2 g/cm). Under pressure, the network structure of SiO_2 glass changes significantly. Several experimental techniques such as Brillioun (Grimsditch, 1986), Raman (Hemley, et al., 1986), infrared (Williams & Jeanloz, 1988), neutron and x-ray scattering(Meade, et al., 1992; Susman et al., 1991), have been used to investigate the influence of pressure on silica glass. Results obtained reveal an irreversible densified structure in glass samples recovered after being subjected to a pressure of 17 GPa. On the modelling side, atomistic molecular dynamics (MD) simulations demonstrated the existence of density maximum (Jin, 1995; Jin, et al., 1992; Kien, et al., 2020; Wu, et al., 2012). Molecular dynamics (MD) simulation is a computational technique used to study the behavior of atoms and molecules over time (Rapaport, 2004). In the case of silicon dioxide (SiO_2) glass, MD simulations can provide insights into its structural properties, thermal behavior, mechanical properties, and other dynamic processes (Igwe & Batsari, 2022). It has been extensively used in many research studies on silica glass due to its

advantage in studying atomic structure and mechanical properties. Recently, Murakami, et al. (Murakami et al., 2019), carried out MD simulation measurement of the static structure factor and pair distribution of SiO_2 glass subjected to pressure. With increasing pressure, the height of the FSDP decreases and its position shifts to higher values of q. Around 42 GPa, the first sharp FSDP almost disappears. At a pressure of 28 GPa, a peak appears at 3.18 $Å^{-1}$. This peak grows with an increase in pressure. The pressure has little influence on S(q) at higher values of q.

In this study, MD simulations were used to study the structural transformations in densified silica glass. The BKS potential was used because the potential could reproduce several high-temperature structural transformations of silica glass at reasonable densities when compared with experiment. The pair distribution function was calculated at varying densities. Next, the distribution of bond angle were analyzed at each point. Finally, we discuss the dominant structural mechanism occurring under high density.

MATERIALS AND METHODS

Computational Detail

Interatomic Potential and Simulation Procedure

To perform a molecular dynamics simulation, it is necessary to have a potential which is able to describe the geometry reliably. For the case of SiO_2 glass, the widely used BKS (van Beest, Kramer, and van Santen) potential has proven to describe amorphous silica reliably. The formation of the BKS potential is shown as follows (van Beest, et al., 1990):

$$V(r_{ij}) = \frac{q_i q_j e^2}{4\pi\epsilon_0 r_{ij}} + A_{ij} e^{-r_{ij}/B_{ij}} - \frac{C_{ij}}{r_{ij}^6} \qquad (1)$$

where q_i is the partial charge of atom i, r_{ij} is the distance between atom i and j. A_{ij}, B_{ij} and C_{ij} are given in Table 1.

Equation (1) is given by the sum of a Buckingham and a long-range Coulombic terms. The presence of the Coulomb part makes the use of such potentials time consuming for large systems since they have to be evaluated by means of approaches like the Ewald summation (Allen & Tildesley, 2017). The code was implemented on Large scale LAMMPS uses reciprocal space fixes to compute the long range interactions, but even then the simulations are still very slow. One possibility to avoid this problem is to use the Wolf summation method proposed by Wolf et al. (Wolf, et al., 1999), in which the Coulomb term is replaced by:

$$\frac{q_i q_j e^2}{4\pi\epsilon_0 r_{ij}} \rightarrow \left\{\frac{q_i q_j e^2}{4\pi\epsilon_0}\left[\left(\frac{1}{r_{ij}} - \frac{1}{r_c}\right) + \frac{r_{ij}-r_c}{r_c^2}\right] \; r < r_c \qquad (2)$$

$$r \geq r_c$$

Where r_c is a cutoff distance on Coulomb interactions. In this form the effective long-range potential becomes thus short ranged by smoothly truncating the potential and hence computationally much more efficient. The parametrization of the BKS model was based on Hartree–Fock calculations of a single SiO_4 tetrahedral, charge-saturated by four hydrogen atoms

Simulation Procedure

The glass structure was obtained by the melt-quench method. The simulation started from a random configuration of 1000 silicon atoms and 2000 oxygen atoms confined in a cubic box. The size of the box is fixed to match the physical density of the glass. The system was then heated up to 8000 K in NVT (constant number of atoms, volume and temperature) ensemble and equilibrated for 100 ps, then the sample was cooled down to 300 K by a temperature step of 2000 K in NPT (constant number of atoms, pressure and temperature) ensemble. The quenched sample was relaxed at 300 K and 0 bar for 150 ps to release the thermal stress. According to previous studies (Vollmayr, Kob, & Binder, 1996), the cooling rate had a great influence on the structure properties and a slow cooling rate was considered to be a better option. Therefore, the cooling rate was set to be 0.2 K/ps in this study. The pair distribution function (PDF) and the bond angle distributions (BAD) were calculated after running for six picoseconds at 293K and were accumulated every ten timesteps for three hundred timesteps.

RESULTS AND DISCUSSION

In Figure 1 we show the pair-distribution functions, g(r) for SiO_2 glasses at the normal (2.2 g/cm^3) and high densities, 3.5 and 4.28 g/cm^3. The first, second and third peak of g(r) represent the average Si-O, Si-Si and O-O bond distances, respectively. For the normal density glass, the first peak in $g(r)_{si\text{-}o}$ gives the Si-O bond length to be 1.61 Å. There is a gap in $g(r)_{si\text{-}o}$ between 1.80 - 2.98 A, a small shoulder around 3.80 Å, and a broad peak at 4.16 Å**.** As the density increases, the position of the first peak in $g(r)_{si\text{-}o}$ remain almost unchanged up to 3.53 g/cm^3. However the gap in $g(r)_{si\text{-}o}$ decreases as the density increases and the second peak shifts to 3.98 Å at 3.53 g/cm^3. At a pressure of 43 GPa where the glass density (4.28 g/cm^3) reaches the density of stishovite, the first peak in $g(r)_{si\text{-}o}$ occurs at 1.68 Å instead of 1.61 Å. In crystalline stishovite, the Si-O bond lengths are 1.76 and 1.81 Å. In the glass at 4.2 g/cm^3, the second peak in $g(r)_{si\text{-}o}$ is at 3.15 Å**,** close to the next-nearest-neighbor Si-O distance (3.20 Å**)** in stishovite.

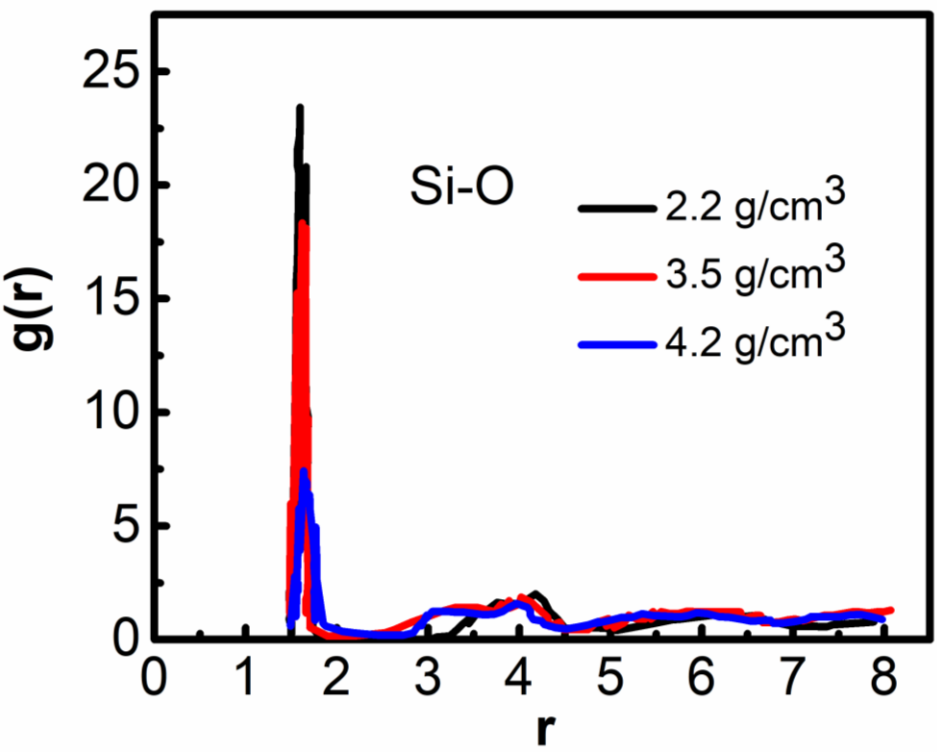

Figure 1: Si-O pair-distribution functions for SiO_2 glasses at normal and high densities at 300 K. Sharp peaks in the figure at 4.2 g/cm^3 correspond to pair-distribution functions for stishovite.

Figure 2(a,b) shows how the Si-Si and O-O pair-distribution functions change upon densification. For the normal density glass, the first peak in $g(r)_{si\text{-}si}$ and $g(r)_{o\text{-}o}$ give the Si-Si and O-O distances to be 3.09 and 2.65 Å, respectively. The second broad peaks in $g(r)_{si\text{-}si}$ and $g(r)_{o\text{-}o}$ give the Si-Si and O-O distances to be 5.03 and 5.06 Å. When the glass density increases to 4.28 g/cm^3, the first peak in $g(r)_{si\text{-}si}$ splits into two peaks. One of these peaks is located at 2.59 Å, close to the Si-Si distance (2.67 Å A) in the stishovite. The second peak appears at 3.07 Å which is close to the Si-Si distance (3.24 Å) in the stishovite. At normal density. It increases to 10 at 3.53 g/cm^3 and to 12 at 4.28 g/cm^3.

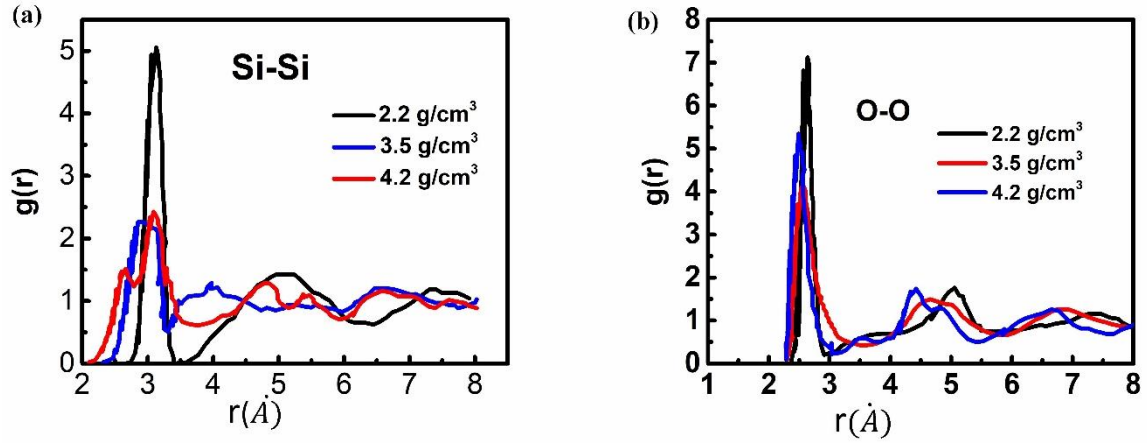

Figure 2: Si-Si and O-O pair-distribution functions for SiO_2 glasses at normal and high densities at 300 K.

Figure 3 displays the MD results for O-Si-O and Si-O-Si bond-angle distributions in SiO_2 glasses at normal and high densities. As the density increases, the peaks in these distributions broaden and also shift to lower angles because of increased distortions of $Si(O_{1/2})_4$ tetrahedra. In the normal density SiO_2 glass, the Si-O-Si bond-angle distribution has a peak at 142^o with a full width at half maximum (FWHM) of peak is 26^o (Fig. 3a). Both of

these results are in excellent agreement with NMR measurements. With a density increase of 33%, this peak shifts gradually to 137°. With 60% densification, the peak moves to 127° and a broad shoulder appears between 135° and 150°. At the stishovite density, the Si-O-Si bond-angle in the glass has broad peaks around 95° and 128°. These values are close to the Si-O-Si angles, 98.65° and 130.67°, in the stishovite crystal. Thus, the results for pair-distribution functions and bond angle distributions at 4.2 g/cm^3 contain strong evidence for distorted $Si(O_{1/3})_6$ octahedra in the glass, joined at corners and sharing edges as well. At normal density, the O-Si-O distribution has a peak at 109° with a full width at half maximum (FWHM) of 10°. With a 20% increase in the density, this peak moves to 107° and the FWHM increases to 12°. A further increase of 40% in the density shifts the peak to 104° and increases the FWHM to 17°. However, there is a dramatic change in the distribution when the glass density reaches the stishovite density: The O-Si-O distribution has broad peaks at 90° and 171°. In the crystalline stishovite on the other hand, the O-Si-O angles are 81.35°, 90°, 98.65° and 180°.

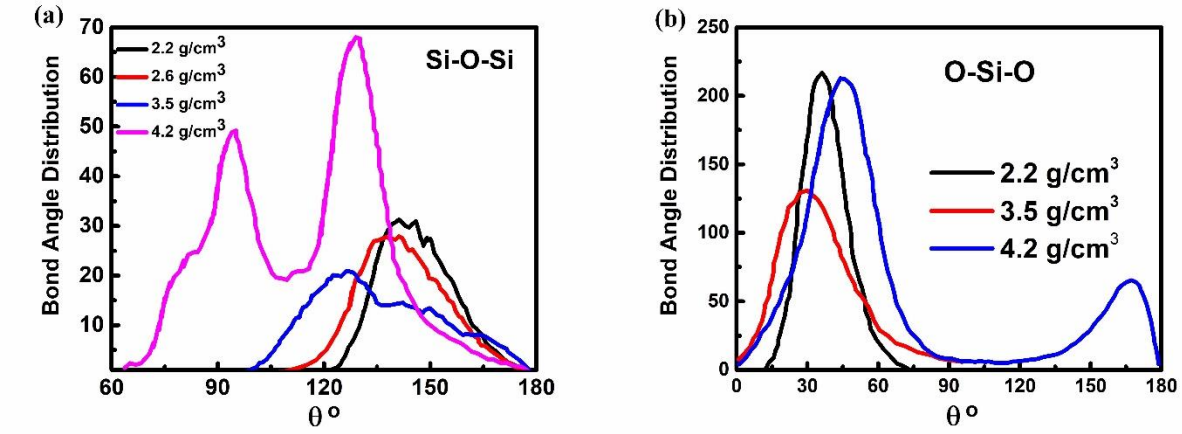

Figure 3: Bond-angle distributions for normal and high density SiO_2 glasses.

CONCLUSION

The microscopic structures in densified SiO2 glasses was investigated using molecular dynamics simulations. The results of pair distribution functions and bond angle distributions show that up to 60% densification the $Si(O_{1/2})_4$ tetrahedral structural unit remains intact and structural change is associated with bending and distortion of the tetrahedral. At high pressure where the glass density reaches the stishovite density the Si-O coordination changes from 4 to 5.8 and the bond length increases from 1.61 to 1.67 A. The O-Si-O angle distribution is peaked at 90° with a full width at half maximum (FWHM) of 21° and the Si-O-Si angle distribution is peaked at 95° and 128°. These results provide firm evidence that the system has transformed from a corner-sharing tetrahedral network to one in which there are corner-sharing and edge-sharing octahedral.

REFERENCES

Allen, M. P., & Tildesley, D. J. (2017). Computer Simulation of Liquids: Oxford University Press.

Brazhkin, V. V., Lyapin, A. G., & Trachenko, K. (2011). Atomistic modeling of multiple amorphous-amorphous transitions in SiO_2 and GeO_2 glasses at megabar pressures. Physical Review B, 83(13), 132103. doi:10.1103/PhysRevB.83.132103

Du, T., Sørensen, S. S., To, T., & Smedskjaer, M. M. (2022). Oxide glasses under pressure: Recent insights from experiments and simulations. Journal of Applied Physics, 131(17). doi:10.1063/5.0088606

Grimsditch, M. (1986). Annealing and relaxation in the high-pressure phase of amorphous SiO_2. Physical Review B, 34(6), 4372-4373. doi:10.1103/PhysRevB.34.4372

Hemley, R. J., Mao, H. K., Bell, P. M., & Mysen, B. O. (1986). Raman Spectroscopy of SiO_2 Glass at High Pressure. Phys Rev Lett, 57(6), 747-750. doi:10.1103/PhysRevLett.57.747

Hong, X., & Newville, M. J. p. s. s. (2020). Polyamorphism of GeO_2 glass at high pressure. 257(11), 2000052.

Igwe, I. E., & Batsari, Y. T. (2022). Atomistic Simulation of the Effect of Temperature on Mechanical Properties of some Nano-Crystalline Metals. African Scientific Reports, 1(2), 95–102. doi:10.46481/asr.2022.1.2.33

Jin, W. (1995). Molecular-Dynamics Simulations of Structural Transformation and Dynamical Correlations in Silica Glass at High Pressures. In Proceedings of the 19th Annual Conference on Composites, Advanced Ceramics, Materials, and Structures—B: Ceramic Engineering and Science Proceedings (pp. 1077-1087).

Jin, W., Kalia, R. K., & Vashishta, P. (1992). Structural and Dynamical Correlations in Stishovite and High Density Silica Glass. MRS Online Proceedings Library (OPL), 293, 247. doi:10.1557/PROC-293-247

Kapoor, S., Wondraczek, L., & Smedskjaer, M. M. (2017). Pressure-Induced Densification of Oxide Glasses at the Glass Transition. 4. doi:10.3389/fmats.2017.00001

Kien, P. H., Trang, G. T. T., & Hung, P. K. (2020). Topological analysis on structural transition under compression and structural heterogeneity in silica glass: a molecular dynamics simulation. Phase Transitions, 93(7), 639-653. doi:10.1080/01411594.2020.1768257

Klinger, M. I. (2013). Glassy disordered systems: Glass formation and universal anomalous low-energy properties: World Scientific.

Machon, D., Meersman, F., Wilding, M. C., Wilson, M., & McMillan, P. F. (2014). Pressure-induced amorphization and polyamorphism: Inorganic and biochemical systems. Progress in Materials Science, 61, 216-282. doi:https://doi.org/10.1016/j.pmatsci.2013.12.002

Meade, C., Hemley, R. J., & Mao, H. K. (1992). High-pressure x-ray diffraction of SiO2 glass. Phys Rev Lett, 69(9), 1387-1390. doi:10.1103/PhysRevLett.69.1387

Murakami, M., Kohara, S., Kitamura, N., Akola, J., Inoue, H., Hirata, A., . . . Ohishi, Y. (2019). Ultrahigh-pressure form of SiO2 glass with dense pyrite-type crystalline homology. Physical Review B, 99(4), 045153. doi:10.1103/PhysRevB.99.045153

Polian, A., & Grimsditch, M. (1990). Room-temperature densification of a- SiO_2 versus pressure. Physical Review B, 41(9), 6086-6087. doi:10.1103/PhysRevB.41.6086

Rapaport, D. C. (2004). The Art of Molecular Dynamics Simulation (2 ed.). Cambridge: Cambridge University Press.

Susman, S., Volin, K. J., Price, D. L., Grimsditch, M., Rino, J. P., Kalia, R. K., . . . Liebermann, R. C. (1991). Intermediate-range order in permanently densified vitreous SiO_2: A neutron-diffraction and molecular-dynamics study. Phys Rev B Condens Matter, 43(1), 1194-1197. doi:10.1103/physrevb.43.1194

van Beest, B. W. H., Kramer, G. J., & van Santen, R. A. (1990). Force fields for silicas and aluminophosphates based on ab initio calculations. Phys Rev Lett, 64(16), 1955-1958. doi:10.1103/PhysRevLett.64.1955

Vollmayr, K., Kob, W., & Binder, K. (1996). Cooling-rate effects in amorphous silica: A computer-simulation study. Physical Review B, 54(22), 15808-15827. doi:10.1103/PhysRevB.54.15808

Williams, Q., & Jeanloz, R. (1988). Spectroscopic evidence for pressure-induced coordination changes in silicate glasses and melts. Science, 239(4842), 902-905. doi:10.1126/science.239.4842.902

Wolf, D., Keblinski, P., Phillpot, S. R., & Eggebrecht, J. (1999). Exact method for the simulation of Coulombic systems by spherically truncated, pairwise r−1 summation. The Journal of Chemical Physics, 110(17), 8254-8282. doi:10.1063/1.478738 %J The Journal of Chemical Physics

Wu, M., Liang, Y., Jiang, J.-Z., & Tse, J. S. (2012). Structure and Properties of Dense Silica Glass. Scientific Reports, 2(1), 398. doi:10.1038/srep00398